ADVANCED ENGINEERING MATERIALS

DOI: 10.1002/adem.200800021

Optimisation of Metallic Fibre Network Materials for Compact Heat Exchangers**

By I. O. Golosnoy, A. Cockburn, and T. W. Clyne*

Compact convective heat exchangers are becoming increasingly important in various areas of application,[1] with highly porous materials or structures offering obvious advantages. However, optimisation of the material and structure is subject to several conflicting requirements. For example, a high internal surface area favours rapid heat exchange with the fluid, but may be associated with a relatively low permeability, inhibiting fluid flow, and increased danger of clogging from foreign material carried by the fluid. This introduces uncertainty about the optimal scale of the porosity. There have been several studies in recent years of the use of highly porous metals as heat exchangers.[2–5] Bonded metal fibre network materials offer advantages for use as heat exchanger cores, since they can be produced by simple and cost-effective routes, with considerable versatility concerning metal composition and network architecture.[6–9]

There have been several previous studies[5,10–14] of porous materials in steady state heat exchange. The heat transfer performance is usually expressed in terms of a Nusselt number, Nu, obtained using a system dimension (such as channel height or length) as the characteristic distance. While this is useful for comparative studies with a given geometry, it is of limited use for material performance assessment, since the overall heat exchange rate does not in general scale linearly with system dimensions. For example, the local rate of lateral heat exchange usually falls off along the length of a system.[15] (Furthermore, there are several dimensions which could be used to obtain a Nu number, including the pore size, exchanger length etc.) In order to obtain an overall Nu number, which is independent of system length,[15] it is necessary to take the mean log temperature ΔT_{lm} as the temperature difference between fluid and surroundings. However, there have been studies[5,11] in which this has not been done, making comparison of results difficult. Also, the surface area available for heat exchange does not scale linearly with porosity level. This makes it difficult to draw general conclusions about the behaviour of porous materials from these experimental results.

In view of the relatively complex interplays between performance, exchanger size and pore (fibre network) architecture, it is difficult to just use experimental data as a guide, and modelling approaches should be explored. The difficulty of identifying geometry-independent parameters characterising the performance suggests that modelling is required of convective and conductive heat transfer for specific geometries, in such a way that figures of merit can be extracted. Several authors have modelled the use of porous materials in convective heat exchange, using both analytical and numerical approaches.[12–14,16] Of course, analytical models are likely to be more tractable and versatile, provided they can be shown to be acceptably accurate. Lu et al.[16] modelled the structure of a wide plate of aluminium foam as a cubic array of solid cylinders. The rate of convection was equated to the rate of conduction to the channel wall, to find the overall heat transfer rate. The overall heat exchange rate, in steady state, was obtained by examining conductive heat flow in the solid and equating the transverse conductive heat flux, the convective heat flux at the foam surface and the rate of thermal energy change in the fluid. Lu et al.[16] arrived at a prediction for the optimal foam density for minimum power consumption, by considering the way heat exchange and flow resistance vary with porosity level. They concluded that the heat exchange performance improves (without limit) as the cell size is increased, with no dependence on foam density. These conclusions are clearly rather counter-intuitive, which may be attributable to their failure to account for the effect of pump performance on the heat exchange rate. For real pumps, the pressure drop is not independent of flow rate.[17] Pump behaviour can be characterised by a curve defining pressure drop as a function of flow rate, with the pressure drop reducing as the flow rate increases. If the pore size is increased, the flow rate required for efficient system operation also increases. When system scale, and therefore flow

[*] Dr. I. O. Golosnoy, Dr. A. Cockburn, Prof. T.W. Clyne
Department of Materials Science & Metallurgy
Cambridge University
Pembroke Street, Cambridge CB2 3QZ, UK
E-mail: twc10@cam.ac.uk

[**] Funding for this work has been provided by EPSRC, through a Platform Grant, and by DTI, via a Technology Programme project involving Avcen Ltd. and Fibretech Ltd. The authors are grateful to Lee Marston, of Fibretech, who supplied the fibres. In addition, there have been a number of productive technical discussions with several members of the committee overseeing the DTI project, notably Jeff Jupp, Mike Dacre, Panos Laskaridis (Avcen) and Mike Winstone (DSTL).

rate, are increased, the pressure drop available from a given pump is reduced. This gives a flow rate lower than that predicted by Lu et al.[16] and correspondingly impaired heat exchange performance. This effect limits the performance of heat exchangers with a coarse structure.

It's therefore clear that, since the performance of a (steady state) heat exchanger is affected by its dimensions, surface heat exchange, core thermal properties, operating temperatures, core permeability and pumping system characteristics, determining the optimal structure is complex and challenging. In the present paper, an analytical model is presented, which allows the dependence of heat exchange performance on fibre network architecture and operating conditions to be examined. Its validity is assessed by comparison with experimental data.

Experimental Procedures

Material Production

Cylindrical fibre network specimens were made by sintering (4 hours at 1200 °C) of stainless steel (type 446) fibres, produced by Fibretech Ltd using a melt extraction process. These fibres have a distorted circular section, with a shape that might be described as resembling a crescent or a kidney. It's convenient to treat the fibres as if they were cylinders, and the appropriate diameter, giving the correct porosity and surface area, is about 40 µm. The fibre orientation distribution was found (using X-ray tomography) to be approximately isotropic. Further details of the microstructure and network architecture are available elsewhere.[7–9]

Heat Flow Apparatus

The heat exchange behaviour of the porous materials was studied using the experimental apparatus shown in Fig. 1. Testing was carried out with a high flow rate of cooling water, such that $T_{s,in}$ and $T_{s,out}$ differed by less than 0.5 °C. Good thermal contact between the tube wall and porous medium was ensured by wrapping the sample in Al foil and applying a layer of high thermal conductivity (3.0 W m^{-1} K^{-1}) heat transfer compound between the foil and tube wall, in order to remove air gaps and improve interfacial conductance.

Air from a compressor was heated to a predetermined temperature, using an in-line process heater, controlled via a digital PID controller (Honeywell) with a K-type control thermocouple located on the downstream side of the heater. Measurements were carried out in the steady state, after allowing 30 minutes for the thermal profile to stabilise. The pressure difference across the sample was measured with a Digitron P200 H digital manometer. Assuming Darcy's law, the specific permeability was calculated from the relationship between flow rate and pressure drop. The latter was determined for flow rates varying from 10–100 litres per minute. For each sample, recordings were repeated three times, and the average value taken.

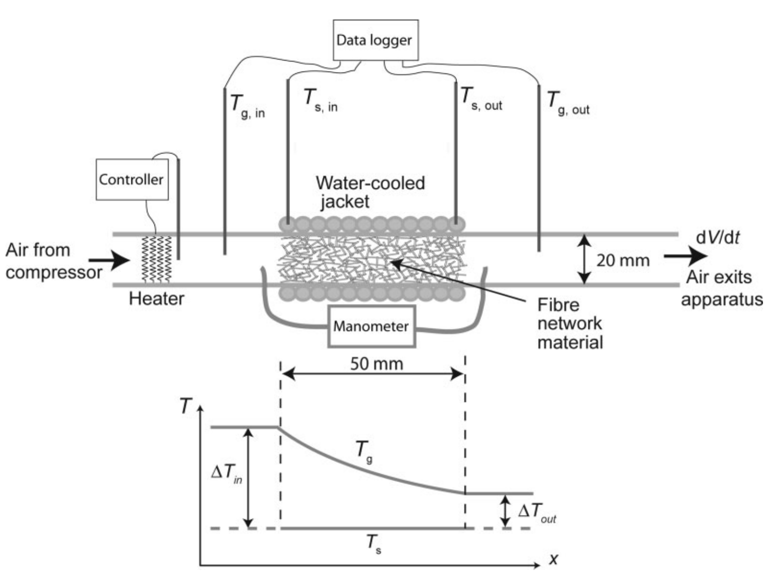

Fig. 1. Schematic depiction of the heat exchange apparatus.

Heat Extraction Rates under Steady State Conditions

The system is described in terms of cylindrical co-ordinates, (x, r, θ), with L being the system length, R the internal radius of the conduit, u the average gas velocity, u_{inside} (= $u/(1\text{-}\phi)$, where ϕ is the fibre volume fraction) the average gas velocity within the fibrous material, $T_{g,in}$ and $T_{g,out}$ the entrance and exit temperatures of the gas and T_s the wall temperature.

By measuring u, $T_{g,\,in}$, and $T_{g,\,out}$, in the steady state, the rate at which heat is being extracted from the gas can be obtained

$$Q = \pi R^2 u \rho_g c_g (T_{g,in} - T_{g,out}) \tag{1}$$

The heat exchange rate per unit volume of heat exchanger material, a key performance parameter, can be expressed as

$$\frac{Q}{V} = \frac{u c_g \rho_g (T_{g,in} - T_{g,out})}{L} \tag{2}$$

Taking gas properties and surface temperature to be constant, the rate of heat exchange is often[15] linearly related to the logarithmic mean temperature difference, ΔT_{lm},

$$\Delta T_{lm} \equiv \frac{\Delta T_{out} - \Delta T_{in}}{\ln(\Delta T_{out}/\Delta T_{in})} \tag{2a}$$

in which, for the present case

$$\Delta T_{out} = (T_{g,out} - T_s), \Delta T_{in} = (T_{g,in} - T_s) \tag{2b}$$

Four sets of experimental data are plotted in the form of (Q/V) against ΔT_{lm} in Fig. 2. It can be seen that these indicate a linear relationship, which suggests that the conditions are amenable to analytical modelling.

The assumption that T_g is independent of r (see later) was investigated experimentally by measuring $T_{g,\,out}(r)$. Its variation between $r = 0$ and $r = R$ was found to be less than 1 °C, confirming the validity of the assumption of negligible radial thermal gradients in the gas.

Modelling of Heat Flow

Model Framework

The model is based on balancing the heat exchange between gas, fibrous material and cylinder walls. The main assumptions are: (i) the system is in a steady-state, (ii) the wall temperature, T_s, is constant, (iii) no viscous heating of the gas, (iv) gas properties are constant, (v) radial thermal gradients in the gas are negligible, (vi) thermal conduction in the axial direction is negligible for both fibre network and gas and (vii) the gas flow velocity within the fibre network is uniform and constant.

Convective heat exchange at the gas/fibre interface is modelled by evaluating a heat exchange coefficient for cylinders in a transverse gas flow. The thermal conduction characteristics of the fibre network have been established in a separate study[18], and the gas permeability was measured as a function of the fibre volume fraction. The heat exchange rate through the wall is based on a Newtonian thermal conductance, h_i, measured experimentally. The elemental volume used in the model is shown in Fig. 3.

Heat Transport in the Gas

The temperature of the gas in the elemental volume is affected by advection, heat exchange with fibres and conduc-

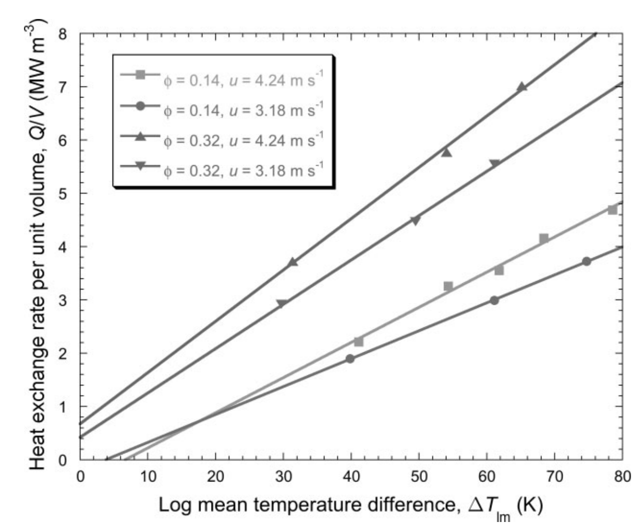

Fig. 2. Variation of volumetric heat exchange rate with log mean temperature difference, for four combinations of fibre volume fraction, φ, and average gas velocity, u.

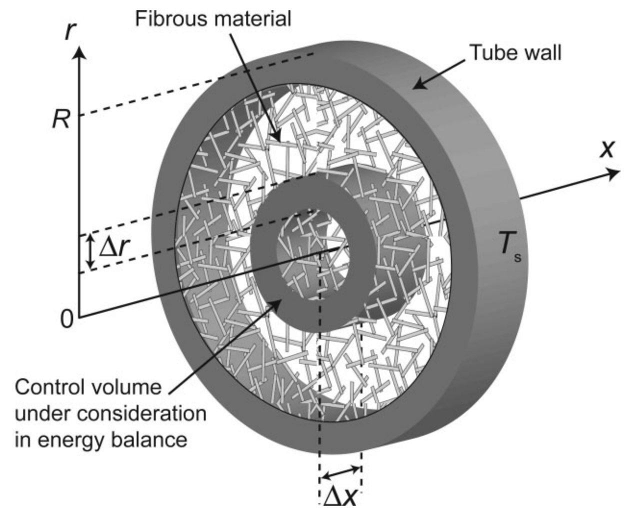

Fig. 3. Elemental volume used in the model.

tion. The change in the thermal energy of the gas within the elemental volume, over a time interval Δt, is given by the difference between the thermal energies of gas entering and leaving the volume, plus the amount of heat exchanged with the surface of the fibrous material, plus the heat conducted in or out of the volume during this period. The energy balance can be re-written in differential form, replacing the local fibre temperature $T_m\ (t,x,r)$ with T_m averaged over the cross-section, from $r = 0$ to $r = R$.

$$\rho_g c_g (1-\phi)\frac{\partial T_g(t,x)}{\partial t} + u\rho_g c_g \frac{\partial T_g(t,x)}{\partial x} + hS\big(\langle T_m\rangle(t,x) - T_g(t,x)\big) = 0 \quad (3)$$

in which

$$\langle T_m\rangle(t,x) = \frac{1}{\pi R^2}\int_0^R T_m(t,x,r)2\pi r\mathrm{d}r \quad (3a)$$

In Eqn. (3), ϱ_g is the gas density, c_g is the gas specific heat capacity, h is the gas/fibre heat transfer coefficient, T_g is the gas temperature, T_m is the fibre temperature, ϕ is the fibre volume fraction, S is the specific surface area of the fibre network material and k_g is the thermal conductivity of the gas. For a steady state, Eqn. (3) reduces to

$$u\rho_g c_g \frac{\partial T_g(x)}{\partial x} + hS\big(\langle T_m\rangle(x) - T_g(x)\big) = 0 \quad (4)$$

In order to solve for $T_g(x)$, an expression is needed for $\langle T_m\rangle(x)$.

Heat Transport in the Fibrous Network

A similar approach can be used for the thermal energy changes taking place in the fibrous material, by considering the effects of radial and axial conduction, and heat exchange with the gas. The balance in this case may be written

$$k_x \frac{\partial^2 T_\mathrm{m}}{\partial x^2} + \frac{k_r}{r}\frac{\partial}{\partial r}\left(r\frac{\partial T_\mathrm{m}}{\partial r}\right) + hS\big(T_\mathrm{g}(t,x) - T_\mathrm{m}(t,x,r)\big) = \phi \rho_\mathrm{m} c_\mathrm{m} \frac{\partial T_\mathrm{m}(t,x,r)}{\partial t} \tag{5}$$

where c_m and ϱ_m are the specific heat capacity and density of the fibres. If axial heat conduction is negligible, and there is a steady state, Eqn. (5) can be simplified to

$$\frac{k_r}{r}\frac{\partial}{\partial r}\left(r\frac{\partial T_\mathrm{m}(x,r)}{\partial r}\right) + hS\big(T_\mathrm{g}(x) - T_\mathrm{m}(x,r)\big) = 0 \tag{6}$$

Since this is a differential equation in r only, and T_g is independent of r, a new variable, $T=(T_m-T_g)$, can be introduced. A substitution can be made for r by defining y as

$$r\left(\sqrt{\frac{hS}{k_r}}\right) = y \tag{6a}$$

allowing Eqn. (6) to be rewritten in standard Bessel form

$$y^2\frac{\mathrm{d}^2 T}{\mathrm{d}y^2} + y\frac{\mathrm{d}T}{\mathrm{d}y} - y^2 T = 0 \tag{7}$$

Solutions to differential equations of this type are well known[19]

$$T = C_1 I_0(y) + C_2 K_0(y) \tag{8}$$

where I_0 and K_0 are Bessel functions, which can readily be evaluated using commercial spreadsheet software, and C_1 and C_2 are constants, which can be evaluated from the boundary conditions. A boundary condition at $r = y = 0$ dictates $C_2 = 0$, while another at $r = R$ gives C_1. Eqn. (8) can then be expressed as

$$T_\mathrm{m}(x,r) = T_\mathrm{g}(x) + \frac{T_\mathrm{w} - T_\mathrm{g}(x)}{I_0\left(R\sqrt{\frac{hS}{k_\mathrm{r}}}\right)} I_0\left(r\sqrt{\frac{hS}{k_\mathrm{r}}}\right) \tag{9}$$

where T_w is the temperature of the fibres where they contact the wall, $T_\mathrm{w} = T_\mathrm{m}$ $(r = R)$, and is constant. The radial conductive flux from the system at x is thus given by

$$q_r(x) = -k_r \frac{\mathrm{d}T_\mathrm{m}(x)}{\mathrm{d}r}\bigg|_{r=R} = \sqrt{k_r hS}\big(T_\mathrm{g}(x) - T_\mathrm{w}\big)\frac{I_1\left(R\sqrt{\frac{hS}{k_\mathrm{r}}}\right)}{I_0\left(R\sqrt{\frac{hS}{k_\mathrm{r}}}\right)} \tag{10}$$

Gas Temperature Distribution and Heat Exchange Rate

The axial temperature profile of the gas is obtained using two assumptions: there is no thermal conduction in the x or r directions and T_g is not a function of r. The expression for $T_\mathrm{g}(x)$ is found by considering heat exchange over the entire cross-section ($0 \leq r \leq R$) for an element of extent Δx in the axial direction. Since the fibre network is at a constant temperature (steady state), the total heat transfer rate into the solid (convective heat exchange with gas), can be equated to the rate of lateral conduction through the wall. Combining Eqns.(4), (6) and (10), the change in gas temperature over the axial distance Δx can be related to the rate of radial conductive flux from the system to give

$$-\frac{\mathrm{d}T_\mathrm{g}}{\mathrm{d}x} = \frac{2\sqrt{k_r hS}}{Ru\rho_\mathrm{g} c_\mathrm{g}} \frac{I_1\left(R\sqrt{\frac{hS}{k_\mathrm{r}}}\right)}{I_0\left(R\sqrt{\frac{hS}{k_\mathrm{r}}}\right)}\big(T_\mathrm{g}(x) - T_\mathrm{w}\big) = \frac{1}{L_\mathrm{eff}}\big(T_\mathrm{g}(x) - T_\mathrm{w}\big) \tag{11}$$

in which the effective exchange length, L_eff, is given by

$$L_\mathrm{eff} = \frac{Ru\rho_\mathrm{g} c_\mathrm{g}}{2\sqrt{k_r hS}} \frac{I_0\left(R\sqrt{\frac{hS}{k_\mathrm{r}}}\right)}{I_1\left(R\sqrt{\frac{hS}{k_\mathrm{r}}}\right)} \tag{12}$$

Eqn. (11) is solved by performing a standard integration

$$T_g(x) = T_\mathrm{w} + \big(T_\mathrm{g,in} - T_\mathrm{w}\big)\exp\left(-\frac{x}{L_\mathrm{eff}}\right) \tag{13}$$

Eqn. (13) implies that the difference between the gas and surface temperature decays exponentially with axial distance, x. Applied for x set equal to the length of the heat exchanger, L, Eqn. (13) can be used to evaluate the exit temperature of the gas

$$T_\mathrm{g,out} = T_\mathrm{w} + \big(T_\mathrm{g,in} - T_\mathrm{w}\big)\exp\left(-\frac{L}{L_\mathrm{eff}}\right) \tag{14}$$

The heat exchange rate per unit volume can be evaluated using Eqns. (2) and (14).

$$\frac{Q}{V} = \frac{uc_\mathrm{g}\rho_\mathrm{g}}{L}\left(1 - \exp\left(-\frac{L}{L_\mathrm{eff}}\right)\right)\big(T_\mathrm{g,in} - T_\mathrm{w}\big) \tag{15}$$

Effect of Lateral Interfacial Thermal Resistance

While T_w refers to the fibres where they contact the internal surface of the container, a more readily measured temperature is that of the coolant, T_s. This is related to T_w via an in-

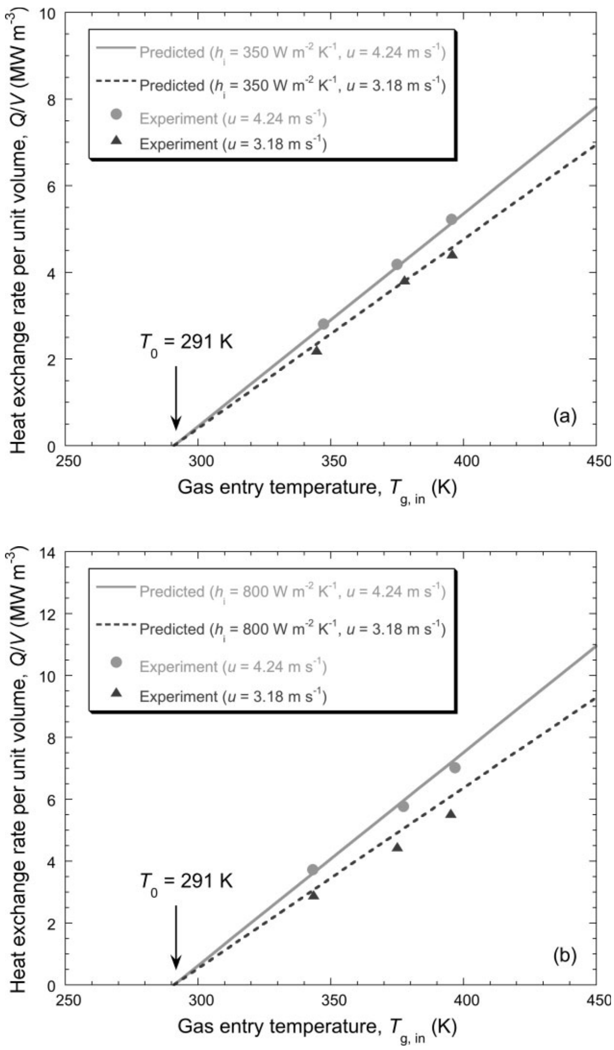

Fig. 4. Comparisons between model predictions and experimental data for the volumetric heat exchange rate, as a function of gas entry temperature, for stainless steel networks with fibre volume fractions of (a) 14 % and (b) 32 %. Data used in the calculations are shown in Table I.

terfacial conductance, h_i. In the steady state, for systems with thin walls, the heat flow rate across the interface will be equal to the network flux at $r = R$

$$Q(x) = q_r(x)|_{r=R}2\pi R\Delta x = h_i(T_w - T_s)2\pi R\Delta x$$
$$= 2\pi R\Delta x H\left(T_g(x) - T_w\right) \quad (16)$$

in which, from Eqn. (10), H is the overall heat exchange conductance, given by

$$H = \sqrt{k_r hS}\frac{I_1\left(R\sqrt{\frac{hS}{k_r}}\right)}{I_0\left(R\sqrt{\frac{hS}{k_r}}\right)} \quad (17)$$

where the meaning of h is defined in §3.2. It follows from Eqn. (16) that

$$T_g - T_w = \frac{h_i}{(h_i + H)}(T_g - T_s) \quad (18)$$

Using this expression to replace (T_g–T_w) in Eqn. (11) leads to an alternative form of the equation for L_{eff}

$$L_{eff} = \left(\frac{H + h_i}{Hh_i}\right)\left(\frac{Ru\rho_g c_g}{2}\right) \quad (19)$$

Heat Exchange between Gas and Fibres

In order to calculate $T_{g,\ out}$, using Eqn. (14), and Q/V, using Eqn. (15), L_{eff} must be evaluated. In order to use Eqn. (19) for this, an expression is required for the surface conductance, h. This can be obtained using an appropriate empirical or semi-empirical correlation expression for the system geometry concerned. The Nusselt number is given by

$$Nu = \frac{hD}{k_g} \quad (20)$$

where k_g is the gas thermal conductivity and D is some characteristic dimension of the system, such as pore size or fibre diameter. An expression for the Nusselt number for a set of cylinders in transverse gas flow[20] is

$$Nu_d \approx 0.5\mathrm{Re}_d^{0.5}\mathrm{Pr}^{0.36} \quad (21)$$

where Nu_d and Re_d are the Nusselt and Reynolds numbers defined using the fibre diameter as the characteristic dimension. Since the Prandtl number term is approximately unity for a gas, and using an expression from Zukauskas[20] to account for the fact that the fibres do not all lie normal to the gas flow, the following equation for h is obtained

$$h = \frac{k_g}{d}0.5Re^{0.5}(1 - 0.54 < \cos^2\theta >) \quad (22)$$

where $<\cos^2\theta>$ is the average value of $\cos^2\theta$, with θ being the angle between the specimen axis and the fibre axis.

Reliability of Conduction Assumptions

It is assumed that axial conduction in both fibres and gas are negligible, in comparison with the convective heat carried by the gas. The diffusional (conductive) heat transfer rate (in $\mathrm{W\,m^{-3}}$) in the axial direction within the gas is given by

$$q_{g,dif} = k_g\frac{\partial^2 T}{\partial x^2} = \frac{k_g}{(L_{eff})^2}(T_{g,in} - T_w)\exp\left(-\frac{x}{L_{eff}}\right) \quad (23)$$

whereas the convective heat transfer rate is given by

$$q_{\mathrm{g,con}} = u\rho_{\mathrm{g}}C_{\mathrm{g}}\frac{\partial T}{\partial x} = -\frac{u\rho_{\mathrm{g}}C_{\mathrm{g}}}{L_{\mathrm{eff}}}\left(T_{g,in} - T_{w}\right)\exp\left(-\frac{x}{L_{\mathrm{eff}}}\right) \tag{24}$$

In the present case, substitution of appropriate data in the expression for the ratio of these two heat transfer rates

$$\left|\frac{q_{\mathrm{g,dif}}}{q_{\mathrm{g,con}}}\right| = \frac{k_{\mathrm{g}}}{L_{\mathrm{eff}}u\rho_{\mathrm{g}}C_{\mathrm{g}}} \tag{25}$$

shows that it's magnitude is less than 10^{-3}, so that axial conduction in the gas can be neglected. A similar conclusion is reached for axial conduction in the fibres.

Evaluation of Interfacial Conductance

In order to estimate the interfacial conductance, h_i, an additional thermal resistance was introduced, using a fibrous layer with a previously-measured conductance.[21] An estimate of h_i was made by dividing the measured heat flux through the system, q, by the additional temperature drop across the interface, ΔT_i. Results from this experiment[18,21] suggested that, for $\phi = 0.14$, $h_i \sim 350$ W m^{-2} K^{-1}. Assuming that the thermal resistance is predominantly between the fibrous material and tube wall, h_i would be expected to vary linearly with ϕ, since the number of fibres in contact with the tube wall would be expected to scale with the fibre volume fraction. If such a relationship is assumed, then experimental data agree well with the model – see below. As expected, the volumetric heat exchange rate increases with gas flow velocity, since both the rate of heat flow into the exchanger and the surface heat exchange co-efficient of the fibrous material, h, increase with flow rate. The heat exchange rate is also dependent on ϕ. This is understandable, since both the surface area available for heat exchange, S, and the radial thermal conductivity, k_r, increase with ϕ.

Predicted and Measured Thermal Characteristics

Effect of Network Architecture

Data used in the calculations are shown in Tables 1 and 2. Noting from Eqn. (15) that Q/V depends strongly on L/L_{eff}, the focus is on the parameters in the expression for L_{eff}. The temperature of the gas gradually approaches the wall temperature, T_s, and the heat exchanger is obviously ineffective when this occurs. For optimum performance, the exchanger length L should be smaller than L_{eff}. In this case, the gas velocity (and its thermal properties) disappear from the final expression (see Eqns. (15) and (19)) and the performance (Q/V) is directly proportional to the overall heat exchange conductance, H, and inversely proportional to the transverse dimension, R. It should also be noted that both h and S depends on the effective fibre diameter (their product being proportional to $d^{-3/2}$). The value of H is now examined as a function of k_r and d, and compared with the interfacial conductance h_i.

The predicted sensitivity of H to both d and k_r is shown in Fig. 5. It can be seen that the sensitivity of H to the transverse dimension R is very weak in all cases. This is because the argument of the Bessel functions in Eqn. (17) is large, for typical fibre arrays. It is also clear that H is rather more sensitive to fibre diameter than to the thermal conductivity of the network. Heat exchanger performance is expected to improve on reducing the fibre diameter (thus increasing the surface area for heat exchange). This is an expected effect, providing the permeability does not drop sufficiently to impair the gas flow - see §4.2. (Of course, in practice there may be other reasons for avoiding a very fine fibre diameter, such as manufacturing and handling difficulties and an increased danger of damage, blockage etc.)

However, for the conditions studied here, (h_i = 350 and 800 W m^{-2} K^{-1}, d = 40 µm, k_r = 0.67–1.5 W m^{-1} K^{-1} and R =10 mm) the predicted values for H, obtained using Eqn. (17), are over 3 kW m^{-2} K^{-1}, so that the overall heat exchange rate is relatively insensitive to the exact values of fibre diameter or network conductivity. According to

Table 1. Data used in figures.

Fig.	ϕ	d (µm)	k_r(W m^{-1} K^{-1})	h_i(W m^{-2} K^{-1})	H(W m^{-2} K^{-1})	L (mm)	R (mm)	S (mm^{-1})
4(a)	0.14	40	0.67	350	Eqs .(17) & (22)	50	10	14
4(b)	0.32	40	1.5	800	Eqs. (17) & (22)	50	10	32
5 d axis	0.14	varies	0.7 & 1.4	–	Eqs. (17) & (22)	50	10 & 100	Eq. (26)
5 k axis	0.14	40 & 80	varies	–	Eqs. (17) & (22)	50	10 & 100	Eq. (26)
6(a)	varies	40	varies with ϕ	$\propto \phi$(300 for ϕ = 0.1)	Eqs. (17) & (22)	50	10	Eq. (26)
6(b)	0.14	varies	0.67	2000	Eqs. (17) & (22)	50	100	Eq. (26)

Table 2. Property data for air.

specific heat capacity, c_g (J kg^{-1} K^{-1})	1005
density, ρ_g (kg m^{-3})	1.2
dynamic viscosity, μ (Pa s)	1.5 10^{-5}
Prandtl number, Pr	0.7
thermal conductivity, k_g (W m^{-1} K^{-1})	0.026

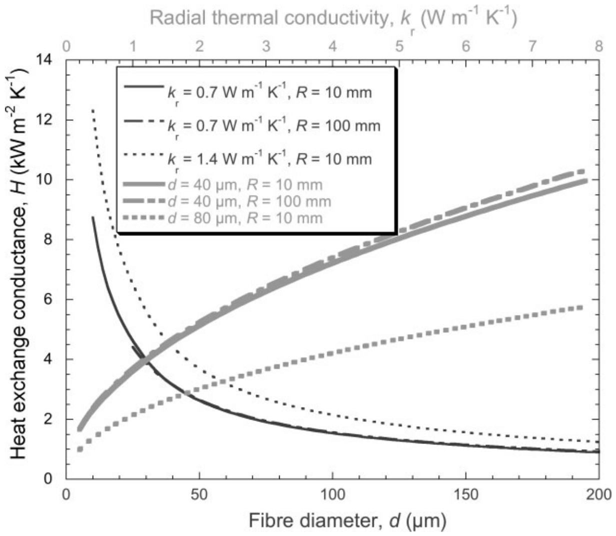

Fig. 5. Predicted dependence (for a 14 % fibre volume fraction steel network material, with a gas inlet velocity of 4.24 m s^{-1}) of the overall heat exchange conductance on the radial thermal conductivity of the fibre network (for fixed fibre diameter) and on fibre diameter (for fixed radial thermal conductivity). Data used in the calculations are shown in Table I.

Eqn. (19), the main limiting factor for heat exchange is the interfacial resistance at the walls. The range of k_r over which this occurs is dependent mostly on the thermal conductance at the tube wall, h_i, but not on the lateral dimensions of the heat exchange system, R. Even if all obvious measures are taken to reduce the contact resistance at the wall[22], it is difficult to imagine that values of h_i greater than 5 kW m^{-2} K^{-1} could be achieved. This being the case, material selection based solely on a high thermal conductivity is not appropriate. Even stainless steel fibre networks, with a relatively low conductivity of k_r ~ 2 W m^{-1} K^{-1}, provide sufficient heat conductance. The 14 % dense networks have a conductivity k_r ~ 0.7 W m^{-1} K^{-1}, which can be increased slighly by improving the inter-fibre bonding[18]. However, performance improvements are expected from improved contact between fibres and wall – for example, brazing may be worthwhile. Increasing h_i from 0.35 to 3 kW m^{-2} K^{-1} is predicted to improve the performance by 400 %, for the conditions being studied here.

When operating with a constant gas flow rate, the effect of fibre volume fraction, ϕ, and diameter, d, can be predicted, taking into account the effect of ϕ on the radial conductivity, k_r, the specific surface area, S, and the internal gas velocity, u_{inside}. The model predicts that the heat exchange rate will increase with increasing ϕ. This effect is intuitive and is confirmed by experiment (Fig. 4). It is due to the increase in S and k_r. However, it should be noted that this is based on treating the fibres as isolated cylinders, so that S increases monotonically with increasing ϕ.

$$S = \frac{4\phi}{d} \tag{26}$$

This is probably valid up to ϕ ~ 0.4. At high values of ϕ, S must start to fall with increasing ϕ. The treatment presented here is thus only valid up to fibre volume fractions of around 40%, but in practice this is the range of prime interest.

Effect of Network Permeability

An increase in flow resistance is expected as d is reduced, and as ϕ is increased. In order to examine the effect this reduction in permeability is likely to have on the heat exchange performance of a real system, it is necessary to consider the characteristics of the pump used to provide the gas flow. In general, the pressure which a pump can provide decreases with increasing flow rate. In order to illustrate this, consider a pump[9] for which the output pressure varies linearly with flow rate, from a maximum value at u = 0 to 0 at $u = u_{\max}$.

$$\frac{\partial P}{\partial x} = \left(\frac{\partial P}{\partial x}\right)_0 - C u_g \tag{27}$$

This allows the flow rate resulting from the combination of a given pump and a heat exchange system to be determined using the following equation.

$$u_g = \left(\frac{\partial P}{\partial x}\right)_0 \left[\frac{\mu\phi}{\kappa} + C\right]^{-1} \tag{28}$$

where μ is the gas viscosity and κ is the permeability of the network. Experimentally measured κ values generally agree well with the Carman-Kozeny relation,[23] which is used here in the following form.

$$\kappa = \frac{(1-\phi)^3}{80\phi^2} d^2 \tag{29}$$

The predicted effect of ϕ on the heat exchange performance is shown in Fig. 6(a), while Fig. 6(b) shows the effect of d ($P_{\max} = 10^4$ Pa, $\mu_{\max} = 8$ ms^{-1}). It can be seen that there is an optimum ϕ, for a given set of operating conditions, giving the best compromise between high surface area and lateral conductivity (favoured by a high value of ϕ) and high heat exchange conductance and gas flow rate (favoured by a low value). For comparative purposes, the effect of having a constant pumping power (pressure drop × volumetric flow rate), rather than the assumed pump curve, is also included. It can

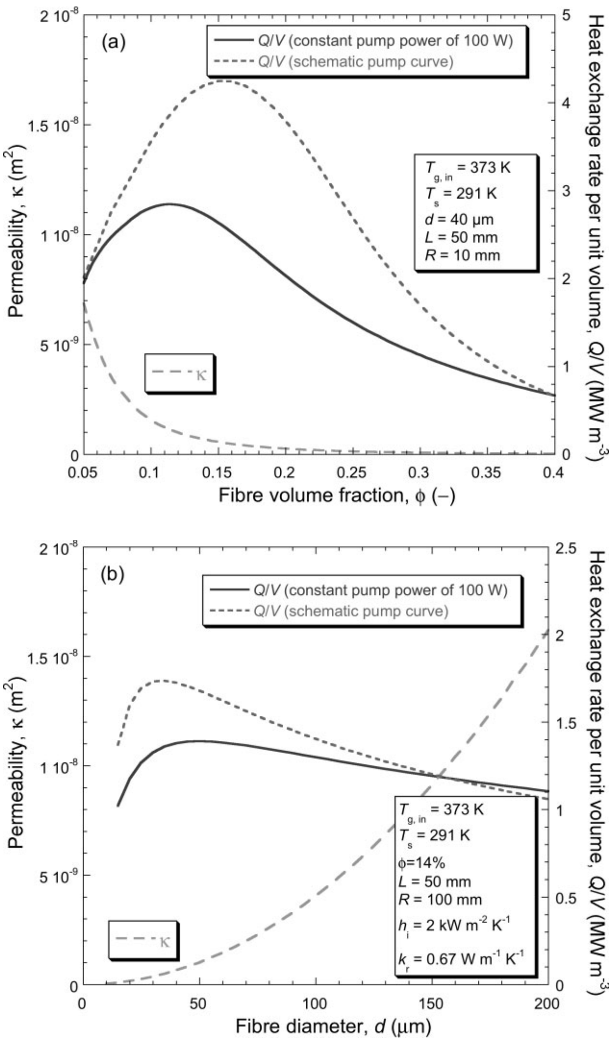

Fig. 6. Predicted dependence of network permeability and volumetric heat exchange rate on (a) fibre volume fraction and (b) fibre diameter. Data used in the calculations are shown in the legend and in Table I.

be seen that the details of the pumping system do affect the predictions, but the broad behaviour is relatively insensitive to this. The optimum ϕ value is of the order of 10–15 %. Fig. 6(b) shows that there is also likely to be an optimum d, but the sensitivity to this variable is somewhat weaker than for the fibre volume fraction. Diameters of the order of 30–100 µm are likely to be most effective, although somewhat coarser fibres are unlikely to have a much lower efficiency. Finer fibres than this, however, are likely to be ineffective, since the associated drop in permeability starts to dominate the behaviour. Of course, this takes no account of the fact that finer structures are also likely to be more prone to blockage and clogging, which would accentuate the effect.

It can be seen from Fig. 6 that the optimal fibre diameter is likely to be dependent on fibre volume fraction, and vice versa. The net effect is best visualised in a contour plot, in which the effect of varying both ϕ and d can be simultaneously examined. This is shown in Fig. 7. The maximum volumetric heat exchange rate value in this plot is actually about

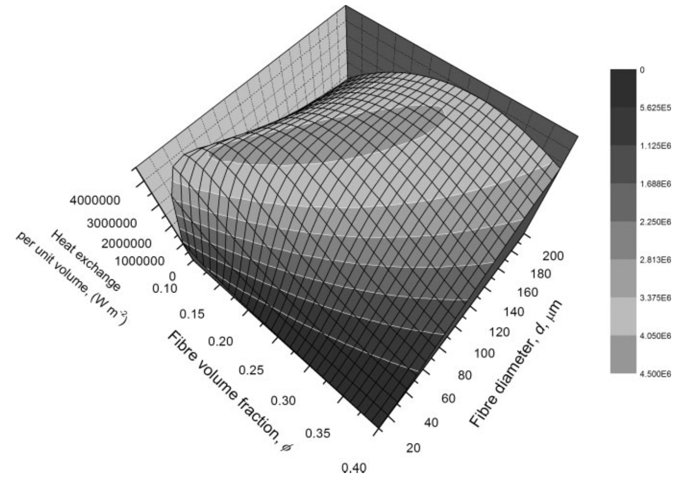

Fig. 7. Contour plot, showing the effect on the volumetric heat exchange rate of varying both fibre diameter and fibre volume fraction, under a given set of operating conditions. P_{max} = 5000 Pa, μ_{max} = 5 m s^{-1}, L = 50 mm; R = 50 mm.

4.2 MW m^{-3} (for d~100 µm and ϕ ~ 0.20). However, the whole of the (dark-shaded) region in the highest range is above 4.05 MW m^{-3}, so it is clear that the peak is not a sharp one, and various combinations of fibre volume fraction and diameter give similar efficiencies in this regime. Nevertheless, it can be seen that the combinations are constrained – for example, if the fibre volume fraction is low, then fine fibres are required. It should also be noted that other issues may be relevant. For example, if a lightweight system is required, then a combination of fine fibres and low fibre volume fraction is preferable. On the other hand, if ease of manufacture, robustness in service and resistance to clogging are important, then coarser fibres and a higher fibre volume fraction may be advisable.

Conclusions

The following conclusions can be drawn from this work.

- A heat exchanger, operating under uniform surface temperature conditions, has been constructed and used to explore the performance of heat exchanger materials based on bonded networks of metallic fibres. The only heat transfer fluid used in this work was air. It was found that the rate of heat exchange is linearly proportional to the log mean temperature difference.
- A new analytical model is presented for heat exchanger performance, giving the rate of heat exchange per unit volume of material, for given dimensions and operating conditions.
- The model predictions indicate that the exchange rate tends to be sensitive to heat transfer conditions at the containing walls. For a heat exchanger core which would be permanently in place, brazing (which would enhance this transfer) is likely to be worthwhile.
- The dependence of heat extraction rates on lateral thermal conductivity has also been examined. The performance gains achievable by using fibres with a very high thermal

COMMUNICATIONS

conductivity (such as copper or silver) are relatively small for typical system dimensions and conditions. Use of a cheaper material, such as (stainless) steel is likely to be more appropriate.

– Taking into account the probable characteristics of the (gas) pumping system, a study has been made of the predicted effects on the heat exchange efficiency of varying the fibre diameter and volume fraction. The efficiency is more sensitive to the fibre volume fraction than to the fibre diameter, although both have an effect, and optimum values for both can be identified, under given conditions. The model may therefore be useful in the design of heat exchanger systems based on gas flow through fibre network materials.

[1] J. E. Hesselgreaves, *Compact Heat Exchangers*, Pergamon, Oxford, **2001.**

[2] B. V. Antohe, J. L. Lage, D. C. Price and R. M. Weber, *Int. J. Heat Fluid Flow* **1996**, *17*, 594.

[3] D. Angirasa, *Int. J. Heat & Mass Transf.* **2002**, *45*, 919.

[4] W. H. Hsieh, J. Y. Wu, W. H. Shih and W. C. Chiu, *Int. J. Heat & Mass Transf.* **2004**, *47*, 5149.

[5] K. Boomsma, D. Poulikakos and F. Zwick, *Mech. Mater.* **2003**, *35*, 1161.

[6] F. Delannay, *Int. J. Solids Structures* **2005**, 2265.

[7] T. W. Clyne, A. E. Markaki and J. C. Tan, *Comp. Sci. Tech.* **2005**, *65*, 2492.

[8] J. C. Tan, J. A. Elliott and T. W. Clyne, *Adv. Eng. Mater.* **2006**, *8*, 495.

[9] T. W. Clyne, I. O. Golosnoy, J. C. Tan and A. E. Markaki, *Phil. Trans. Royal Society A – Mathematical, Physical & Eng. Sciences* **2006**, *364*, 125.

[10] W. J. Mantle and W. S. Chang, *J. Thermophysics Heat Transf.* **1991**, *5*, 545.

[11] J. Tian, T. Kim, T. J. Lu, H. P. Hodson, D. T. Queheillalt, D. J. Sypeck and H. N. G. Wadley, *Int. J. Heat Mass Transfer* **2004**, *47*, 3171.

[12] J. J. Hwang, G. J. Hwang, R. H. Yeh and C. H. Chao, *J. Heat Transfer* **2002**, *124*, 120.

[13] V. V. Calmidi and R. L. Mahajan, *J. Heat Transfer* **2000**, *122*, 557.

[14] K. Ichimiya, *J. Heat Transfer* **1999**, *121*, 978.

[15] F. P. Incropera and D. P. Dewitz, *Fundamentals of Heat and Mass Transfer*, John Wiley & Sons, **2002.**

[16] T. J. Lu, H. A. Stone and M. F. Ashby, *Acta Mater.* **1998**, *46*, 3619.

[17] U. Drofenik, G. Laimer and J. W. Kolar, *IEEE Transactions on Power Electronics* **2005**, *20*, 704.

[18] A. Cockburn, *Thermal Properties of Metallic Fibre Network Material*, PhD thesis, University of Cambridge, **2007**.

[19] J. Davies, *Mathematical Methods for Mathematicians, Physical Scientists and Engineers*, John Wiley & Sons, New York, **1982.**

[20] A. Zukauskas, *Convective Heat Transfer in Cross Flow, Chap 6*, in Handbook of Single-Phse Convective Heat Transfer, S. Kakac, S. R. K and A. Aung (ed.), Wiley, New York, **1987**,

[21] J. C. Tan, S. A. Tsipas, I. O. Golosnoy, S. Paul, J. A. Curran and T. W. Clyne, *Surf. Coat. Techn.* **2006**, *201*, 1414.

[22] R. Holm, *Electric Contacts*, Springer-Verlag, New York, U.S., **1967.**

[23] P. Carman, *Flow of Gases Through Porous Media*, Butterworths Scientific Publications, London, **1956**.

